Enhanced tensile performance of aluminium/composite bonded joints through semi-circular surface modification and stacking sequence optimization

Touati Benali Abdelaziz[1,2], Habib Achache[1,3], Leila Belkhodja[1], Mohammed Benyettou[4], Kouider Madani[4], Benaicha Abdelkader[1,2], Benefissa Noureddine[1,2]

.

[1]*Institute of maintenance and industrial safety, University of Oran2 Mohamed Ben Ahmed, B.P 1015 El M'naouer 31000 Oran, Algeria;*

[2]*Production engineering and industrial maintenance laboratory, LGPMI*

[3]*Laboratory of Mechanics and physics of materials, LMPM, Mechanical Engineering Department, Djilali Liabes University of Sidi-Bel-Abbes, BP 89, Sidi Bel Abbes 22000, Algeria*

[4]*Laboratory of Mechanics of Structures and Solids, LMSS, Mechanical Engineering Department, Djilali Liabes University of Sidi-Bel-Abbes, BP 89 Sidi Bel Abbes, 22000, Algeria*

Enhanced tensile performance of aluminium/composite bonded joints through semi-circular surface modification and stacking sequence optimization

Abstract

This study investigates the combined influence of bonding zone geometry, composite type, and stacking sequence on the tensile strength of aluminium/composite bonded joint using the adhesive Adekit A140. Two surface geometries were considered: a flat bonding zone and a structured rectangular zone, each with or without a semi-circular notch of 0.2 mm at the bottom of the aluminium external surface, aimed at improving stress distribution, delaying debonding, and enhancing tensile strength. These geometries were combined with two types of reinforcements (carbon/epoxy and aramid/epoxy) and four stacking sequences. The results show that adding a semi-circular notch to a flat geometry improves the ultimate load due to more uniform stress distribution. In contrast, the rectangular geometry, although generally beneficial for composites, exhibits less favourable interaction under certain modifications. Among the simulated configurations, the carbon/epoxy assembly with stacking sequence S4 and the flat bonding zone (without modification). These numerical findings provide valuable design optimization and strength recommendations, as well as guiding future experimental studies aimed at confirming these findings.

Keywords: aluminium/composite, bonded joint, CZM, debonding, semi-circular notch.

Introduction

In recent years, the bonded assembly of aluminum and composites has emerged as a lightweight, high-strength solution that is particularly valued in the aerospace and automotive sectors. Despite its apparent simplicity, it poses a significant design challenge: the two materials with their markedly different mechanical behaviors need to interact with each other while preventing adhesive failure under tensile loads.

Several studies have established a better understanding of adhesive bonded assemblies [1-5] have investigated how adhesive thickness and geometric variations influence the mechanical performance of these structures. [6-8] then developed predictive models for single-lap joints based on experimental results and numerical simulations. However, methods of reducing stress have also been explored by Barbosa et al [9] demonstrated that optimizing adhesive fillets can effectively reduce peel stress concentrations. Akpinar et al. [10] showed that fillets and chamfers can enhance flexural performance. Zielecki et al. [11] emphasized that the size and radius of chamfers have a significant impact on fatigue durability. Heidarpour et al.[12] revealed that integrated 2D/3D defects within the joint can substantially reduce its load-bearing capacity.

The Cohesive Zone Method (CZM) is one of the most widely used modelling approaches for adhesive layer debonding. Numerous studies have highlighted its efficacy in accurately predicting and characterizing adhesive failure mechanisms [13-17]. Silva et al. [18] have successfully applied this method to scarf joints, enhancing its predictive capability by combining CZM with advanced techniques such as the extended finite element method (XFEM). Benyettou et al. [19] analyzed the load-displacement responses of composite patch-repaired structures in order to assess their mechanical performance and the local damage mechanisms within the adhesive layer. Similarly, Araújo et al. [20] confirmed CZM's capacity to simulate progressive failure with high accuracy. Researchers have also analyzed the behavior of hybrid-repaired or assembled structures. For example, Suwanpakpraek et al.[21] investigated the failure of composite-metal bonded joints using numerical and experimental methods, and analyzed the effect of transition geometries in bonded assembly regions. Solmaz and Turgut [22] examined the effect of taper angles and overlap length on stress distribution and failure in bonded joints.

The aim of this study is to establish a comprehensive optimization methodology for bonded aluminum/composite assemblies by investigating the combined effects of bonding zone geometry, composite type, stacking sequence and a semi-circular notch through 3D simulations conducted in Abaqus. Two bonding geometries are considered (flat and structured rectangular), in both cases with and without a 0.2 mm semi-circular notch at the bottom of the aluminum substrate. These geometries are combined with two types of composite reinforcement (carbon/epoxy and aramid/epoxy) and four stacking sequences ($[0]_8$, $[0/90/0/90]_s$, $[0/45/-45/90]_s$ and $[0/0/90/90]_s$). The semi-circular notch improves stress distribution by ensuring that the central part of the bonding zone remains intact, thereby avoiding stress concentrations at the edges of the overlap length. Adding a semi-circular notch reduces these edge stress concentrations, resulting in a more uniform stress distribution and enhanced ultimate load capacity. Therefore, our objective is to accurately quantify the influence of these parameters on stress distribution and ultimate load, providing designers with practical guidelines to maximize the performance of bonded assemblies.

Geometric modeling and mechanical properties

A single-lap joint configuration consisting of two adherends was investigated: an aluminum substrate made of AL2024-T3 alloy and a composite laminate substrate. The geometric parameters of the SLJ are as follows: length $L = 100\ mm$, width $W = 25\ mm$, overlap length 25 mm and thickness t = 2 mm. The bonding area was created using an ADEKIT A-140 epoxy adhesive with the following dimensions: length $L_{ad} = 25\ mm$, width $W = 25\ mm$, and thickness $t_{ad} = 0.2\ mm$ (Figure 1).

To study the effect of bonding geometry on joint performance, the overlap region was modified geometrically. Two configurations were considered: a flat and a rectangular profiled interface. The flat configuration represents the conventional SLJ, whereas the rectangular profiled configuration has regular rectangular shapes on the adhesive-aluminum interface to improve adhesion (see Figure 1).

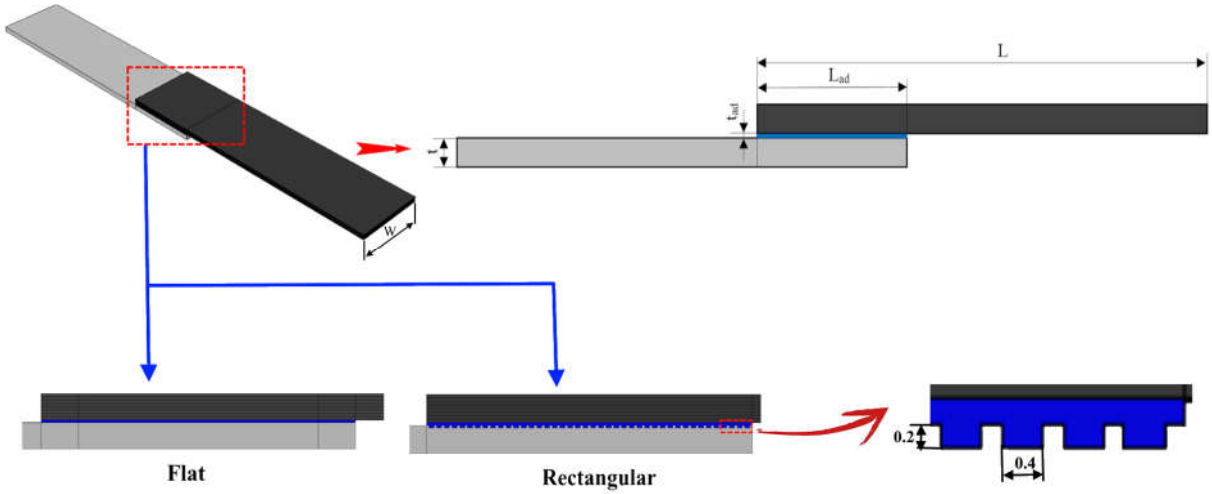

Figure 1. Geometric configurations and dimensions of SLJ models.

The mechanical properties of aluminum, which is widely used in various applications, have a significant impact on its behavior when subjected to loads. In this study, the mechanical properties of aluminum and the adhesive were taken from the experimental work of Madani et al. [23]. Table 1 presents these properties as revealed by their investigation into the mechanical behavior of these materials.

Table 1. Mechanical properties of the aluminum alloy 2024-T3 and Adekit A-140 adhesive [23]

Materials	Aluminium 2024-T3	Adekit A-140
Young's modulus (GPa)	75	2.69
Poisson's ratio υ	0.3	0.3

Table 2. Mechanical properties of the composite material [24]

Materiel	E_1 (Gpa	E_2	E_3	G_{12}	G_{13}	G_{23}	v_{12}	v_{13}	v_{23}
Carbon-epoxy	109	8.819	8.819	4.315	4.315	3.2	0.342	0.342	0.38
Aramid-epoxy	76	5.5	5.5	2.3	2.3	2.3	0.34	0.34	0.34

Numerical analysis

A numerical analysis was performed to evaluate the combined impact of bonding geometry, composite type and fiber orientation on the performance of aluminum/composite single-lap joints. The analysis focused on understanding the impact of geometrical modifications and

laminate configurations on stress distribution, damage initiation, and the joints' overall load-bearing capacity.

Two aluminum surface geometries were examined: a flat interface and a rectangular profiled interface. The profiled configuration was created to improve mechanical bonding and enhance adhesive performance. In both models, a 0.2 mm semi-circular notch was created on the lower substrate of the aluminum of the overlap region to promote a more uniform stress distribution, reduce edge stress concentrations and increase the ultimate strength of the joint.

The upper adherend consisted of laminated composites made from either carbon/epoxy or aramid/epoxy materials. Each laminate consisted of eight orthotropic plies, and four stacking sequences were examined to capture various stiffness and failure behaviors: $[0]_8$, $[0/90/0/90]_s$, $[0/45/-45/90]_s$ and $[0/0/90/90]_s$.. These configurations were chosen as they represent the unidirectional, cross-ply and quasi-isotropic arrangements commonly used in structural applications.

Numerical modelling was performed using ABAQUS/Standard based on a 3D finite element method. Both the aluminum and composite substrates were modelled using C3D8R solid elements (eight-node, linear brick elements with reduced integration). The adhesive layer was modelled using COH3D8 cohesive elements, in accordance with the cohesive zone model (CZM) approach. This approach captures the traction-separation behavior of the adhesive and enables the simulation of the initiation and progressive evolution of interfacial damage under mixed-mode loading. A refined mesh was applied in the overlap region and through the adhesive thickness to accurately capture local stress variations (Figure 2).

The boundary conditions involved fully constrain one end of the aluminum substrate, while applying a 5 mm displacement to the opposite end of the composite adherend along the X-axis. This represents the uniaxial tensile loading direction.

Figure 2. Finite element mesh for adhesive joint

Adhesive modelling

The Cohesive Zone Model (CZM) technique was used to precisely simulate the damage initiation and propagation within the adhesive layer. The CZM is a numerical method that is recognized for its ability to model debonding processes at adhesive layers based on a traction–separation law.

Before any damage occurs, the adhesive layer exhibits elastic behaviour in response to a linear traction-separation relationship, which is determined by a stiffness matrix K. The general form of the constitutive equation is as follows :

$$\begin{Bmatrix} T_n \\ T_s \\ T_t \end{Bmatrix} = \begin{bmatrix} K_{nn} & K_{ns} & K_{nt} \\ K_{ns} & K_{ss} & K_{st} \\ K_{nt} & K_{st} & K_{tt} \end{bmatrix} . \begin{Bmatrix} \varepsilon_n \\ \varepsilon_s \\ \varepsilon_t \end{Bmatrix}$$

The degradation of the adhesive layer is initiated by a quadratic stress criterion, which considers the combined effect of normal and shear stresses. Damage initiates once the following condition is reached:

$$\left(\frac{T_n}{T_n^0}\right)^2 + \left(\frac{T_s}{T_s^0}\right)^2 + \left(\frac{T_t}{T_t^0}\right)^2 = 1$$

The progressive degradation and debonding of the adhesive layer eventually occur due to an energy-based failure law that considers mixed-mode loading. The damage evolution is defined by the energy release rate G_c :

$$G_c = G_{IC} + (G_{IIC} - G_{IC}).\left(\frac{G_s}{G_T}\right)^n$$
$$G_s = G_{II} + G_{III}$$
$$G_T = G_I + G_s$$

Resultats and discussion

Flat geometry

Stress distribution in Aluminum/Aramid-epoxy bonded joint

Figure 3 presents the maximum principal stresses distribution and the QUADSCRT damage criterion within an aluminum/aramid SLJ with flat geometry and $[0]_8$ fiber orientation. The results show that the maximum principal stress is approximately 574 MPa in the first aramid ply, which is located at the edge of the adhesive layer. This region also demonstrates a QUADSCRT value approaching 1, indicating the initiation of adhesive failure and debonding at the joint extremity. This localized stress concentration emphasizes the importance of the interface region, where the combination of tensile stresses and interfacial shear results in progressive degradation and the ultimate loss of adhesion.

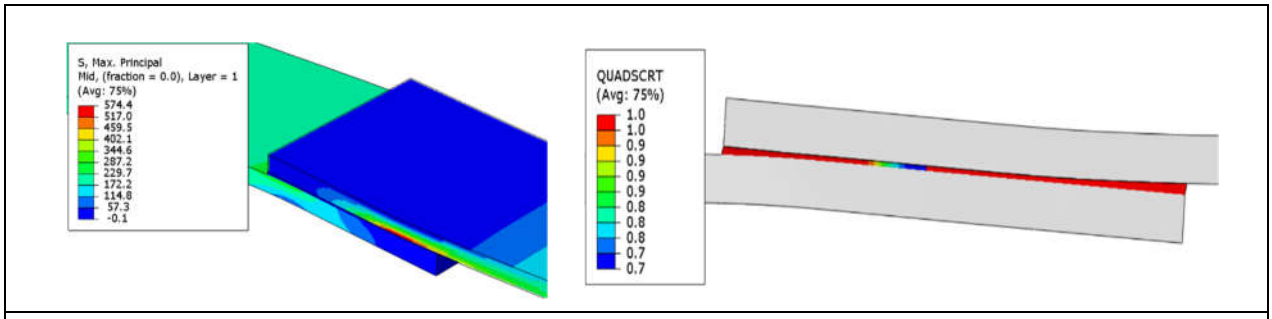

Figure 3. Maximum principal stress and QUADSCRT damage representation for the aluminum/aramid joint.

Stress distribution in Aluminum/Carbon-epoxy bonded joint

Figure 4 shows the distribution of maximum principal stresses in an aluminum/carbon bonded joint with flat geometry and a stacking sequence of $[0]_8$. According to the analysis, the maximum principal stress is approximately 641 MPa in the first carbon ply, which is about an 11% increase compared to the aluminum/aramid configuration. It is the greater stiffness of the carbon fibers that causes this higher stress level, resulting in more efficient load transfer through

the adhesive interface. The QUADSCRT damage analysis shows a larger critical region along the interface where the damage level is high. This suggests that, while carbon can improve the overall stiffness and strengths, it can also induce higher interfacial stress concentrations that may accelerate local damage initiation. These results emphasize the dual effect of carbon reinforcement: enhancing the global load-bearing capacity, but also requiring careful attention to interfacial stress management to ensure durability in the long term.

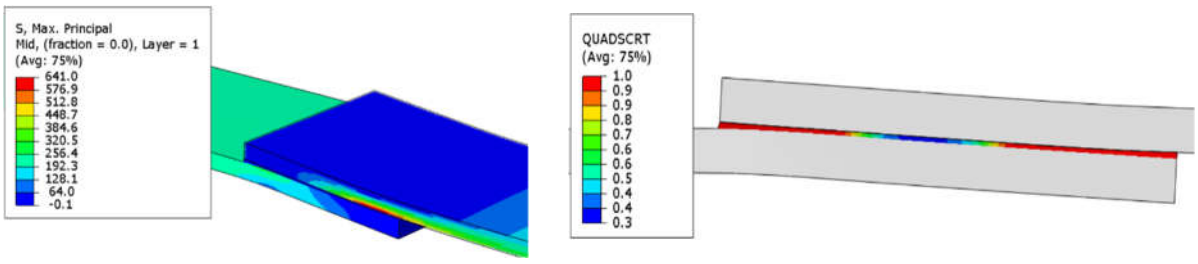

Figure 4. Maximum principal stress and QUADSCRT damage representation for the aluminum/Carbon joint.

Load-displacement comparison

Figure 5 illustrates the load-displacement curves resulting from the tensile analysis of aluminum/composite bonded joints reinforced with either aramid or carbon. The results show that the aluminum/carbon-epoxy configuration has a higher ultimate load capacity, at around 11,060 N, compared to 10,410 N for the aluminum/aramid-epoxy joint. This increase in load-bearing capacity is due to the greater stiffness and better load transfer efficiency of the carbon fibers, which allow for more effective stress redistribution across the bonded area.

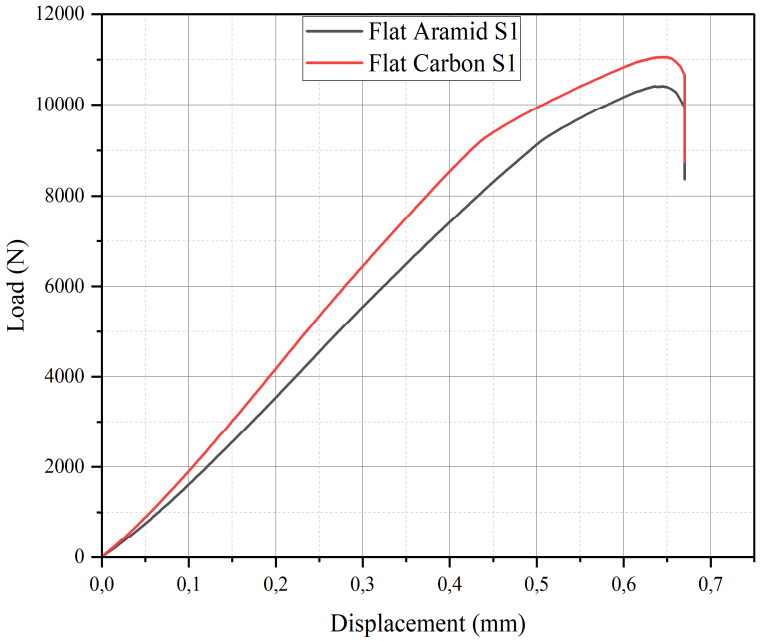

Figure 5. Load-displacement curve for aluminum/aramid and aluminum/carbon joints with flat geometry and $[0]_8$ layup.

The figure 6 shows the distribution of maximum principal stress in each ply of the aluminum/aramid and aluminum/carbon composite assemblies. The highest stress levels are evident in the plies located closest to the adhesive layer.

A comparative analysis of the two configurations reveals that the aluminum/carbon assembly consistently exhibits higher stress values than the aluminum/aramid assembly, particularly in the surface plies. For example, the maximum principal stress in the first ply is 641 MPa for the carbon-reinforced composite and 574 MPa for the aramid-reinforced composite, representing an increase of approximately 11.7%. This observation across various plies emphasizes the superior load-bearing and stress-transmitting capabilities of carbon fibers. This enhanced performance can be attributed to the higher stiffness of carbon fibers relative to aramid fibers, as well as their more linear mechanical response under tensile loading. Overall, however, these results emphasize the significant impact of reinforcement type on the mechanical response of hybrid assemblies, suggesting that carbon fibers could offer enhanced tensile performance in applications where high performance is required.

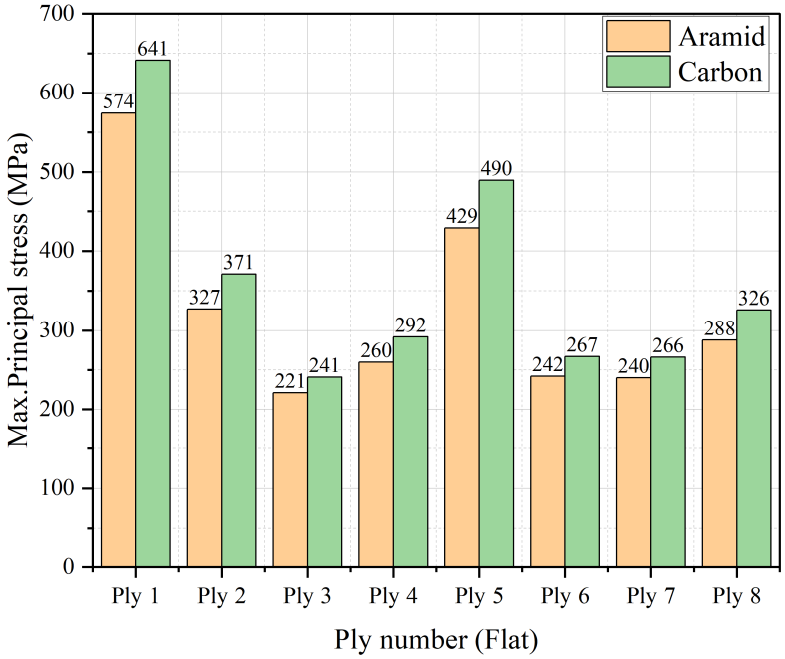

Figure 6. Maximum principal stress in individual plies of aluminum/aramid and aluminum/carbon hybrid joints (flat geometry, $[0]_8$ layup).

Rectangular geometry

Stress distribution in Aluminum/Aramid-epoxy bonded joint

Figure 7 illustrates the distribution of the maximum principal stress and the corresponding QUADSCRT damage factor for an aluminum/aramid joint with rectangular geometry and a $[0]_8$ orientation.The maximum principal stress is approximately 582 MPa in the first aramid ply near the adhesive layer, highlighting a region where there is significant load transfer between the aluminum substrate and the carbon- epoxy substrat. This concentration of stress indicates that the zone where the two materials are joined is critical to the joint's mechanical performance. In parallel, the QUADSCRT damage factor approaches 1 in the same region, indicating the beginning of damage due to tensile loading, which is primarily associated with adhesive debonding. The association between stress localisation and damage evolution confirms the aramid layer's sensitivity to interfacial stresses, emphasising the necessity of an optimised adhesive configuration and fiber orientation to enhance the joint's durability.

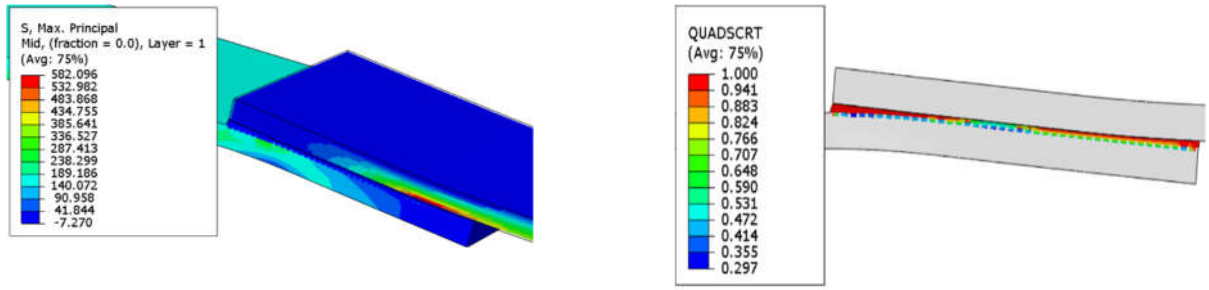

Figure 7. Maximum principal stress and QUADSCRT damage representation for the aluminum/aramid-epoxy joint.

Stress distribution in Aluminum/Carbon-epoxy bonded joint

The maximum principal stress in the first carbon ply is approximately 673 MPa, which is about 15% higher than that achieved with the composite aramid-epoxy. Highlights the carbon fibers enhanced load transfer efficiency, primarily. The increased stress concentration observed near the adhesive layer suggests that the carbon reinforcement significantly improves joint rigidity while ensuring strong interfacial adhesion. Moreover, the QUADSCRT damage factor reaches values close to 1, particularly at the end of the overlap region, indicating that adhesive debonding initiates in these areas due to high local stress gradients (see Figure 8).

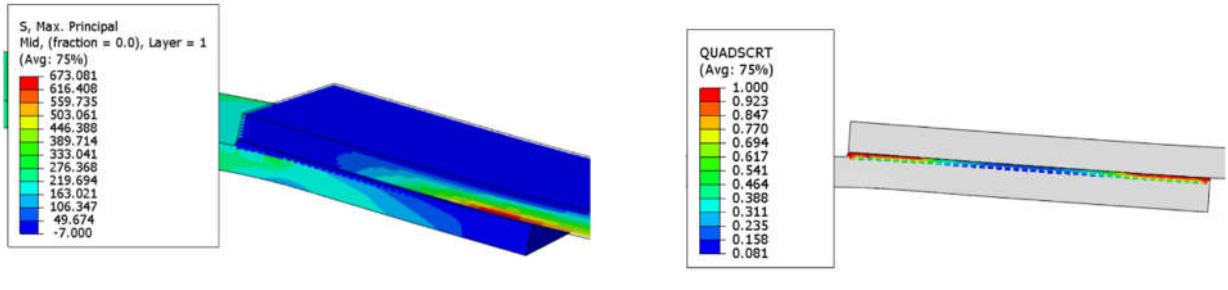

Figure 8. Maximum principal stress and QUADSCRT damage representation for the aluminum/carbon-epoxy joint.

The results of load-displacement behavior, obtained from the FEM analysis of the tensile test on bonded aluminum/composite joints with rectangular geometry and unidirectional $[0]_8$ fiber layup, are presented in Figure 9. Two types of composite reinforcement were examined: aramid/epoxy and carbon/epoxy. As can be seen from the te result, there is a linear elastic response followed by progressive non-linear behaviour up to failure. It is clear from the curves that the aluminum/carbon assembly can support a higher maximum load than the

aluminum/aramid assembly. Specifically, the maximum load achieved by the carbon-reinforced joint is around 11,45 KN, whereas the maximum load achieved by the aramid-reinforced joint is around 9,7 KN. This represents an increase in load-bearing capacity of approximately 18%. This improvement in performance can be explained by the stiffness and strength properties of carbon fibers, which allow for more efficient load transfer across the bonded area. Furthermore, the carbon/epoxy joint exhibits higher displacement at failure, indicating greater energy absorption capacity. In contrast, the aramid/epoxy system fails at a lower load and displacement, indicating a relatively brittle failure mode under the same test parameters.

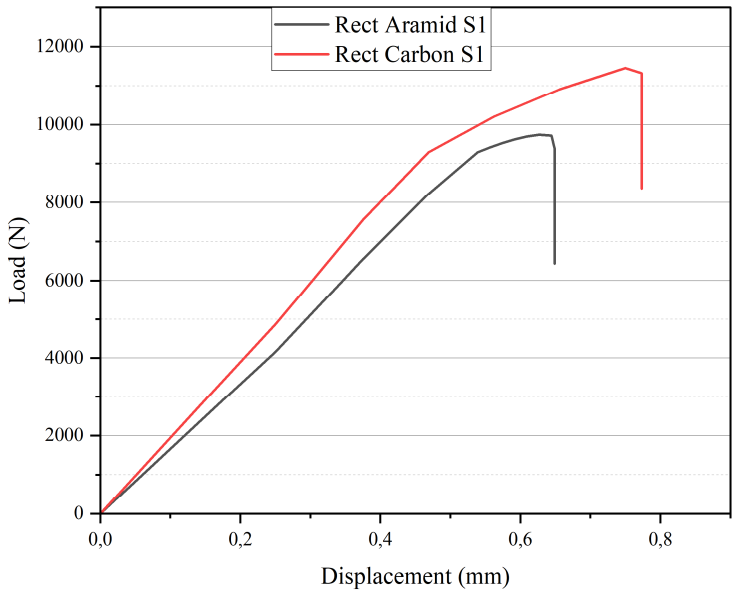

Figure 9. Load-displacement curve for aluminum/aramid and aluminum/carbon joints with rectangular geometry and $[0]_8$ layup.

Figure 10 demonstrates the maximum principal stress distribution in each individual ply of aluminum/composite bonded joints with rectangular geometry and unidirectional $[0]_8$ fiber layup. A clear stress concentration is evident, with the first ply showing the highest stress values in both material types, indicating the adhesive's significant role in load transfer. The carbon/epoxy joint attains a peak stress of 673 MPa in the ply in contact with adhesive layer, whereas the aramid/epoxy equivalent peaks at 582 MPa

This performance difference between carbon and aramid is consistent throughout most plies. The difference in the stress distribution in the layers highlights the stiffness and mechanical compatibility superiority of carbon fibers. the stress distribution further confirms that the first

plies are the structurally most critical, emphasizing the importance of the type of reinforcement and the integrity of the interface in joint design. These results support the idea that carbon fiber composites are more efficient at transferring stress, especially in configurations where geometric structures, such as rectangular design, allow for more uniform load distribution.

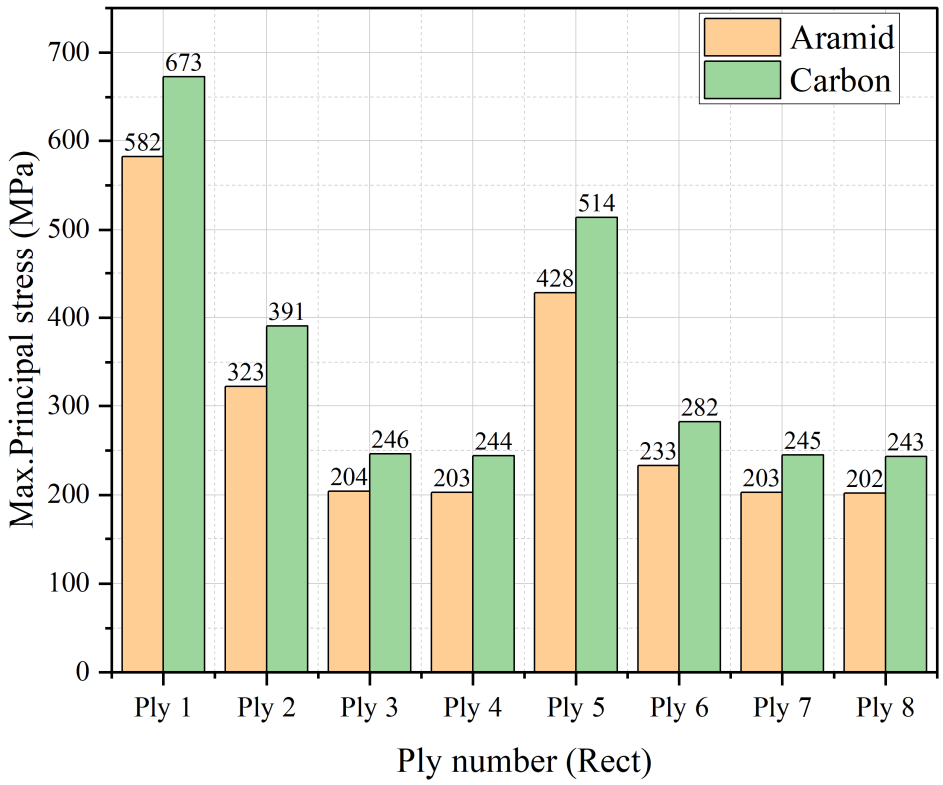

Figure 10. Maximum principal stress in individual plies of aluminum/aramid and aluminum/carbon hybrid joints (rectangular geometry, $[0]_8$ layup).

Stacking sequence effect

This part of our analysis looks at how the ply stacking sequence affects the performance of aluminum/composite bonded joints. The stacking sequence is crucial in influencing the stiffness, stress distribution and failure mechanisms in the bonded joint. The following table summarizes the four representative stacking configurations considered.

Stacking sequence	S1	S2	S3	S4
	$[0]_8$	$[0/90/0/90]_s$	$[0/45/-45/90]_s$	$[0/0/90/90]_s$

The results presented in Figure 11 illustrate how the stacking sequence of the plies influences the tensile strength of aluminum/composite bonded joints with flat and rectangular

configurations. A similar observation can be made in both configurations. the S1 exhibits the maximum load-bearing capacity, while the more varied and multidirectional sequences result in a reduction in tensile strength. In the flat configuration, the S1 achieves maximum loads of 11,060 N and 10,410 N for the aluminum/carbon-epoxy and Aluminum/aramid-epoxy joints, respectively. This is due to the complete fiber alignment along the load direction, which enables efficient load transfer through the adhesive layer and reduces shear stresses between the layers. As the stacking sequence becomes more varied, the maximum load decreases. The S2 configuration achieves 10,230 N for carbon and 9,486 N for aramid, and the S3 sequence demonstrates the lowest resistance. In case of the S4 configuration provides an intermediate performance by combining good stiffness with moderate transverse flexibility.

The same general behavior is observed for the rectangular shaped geometry, but with slightly higher maximum loads. The rectangular geometry improves the bonding area and stress distribution along the adhesive layer, resulting in delayed damage initiation and increased joint stiffness. This effect is particularly noticeable for the S1 and S4 configurations, in which the rectangular geometry ensures a more uniform load transfer. Conversely, for the multidirectional sequences (S2 and S3), the stress redistribution within the composite and adhesive layer leads to an early onset of damage, resulting in lower peak loads compared to S1, S4.

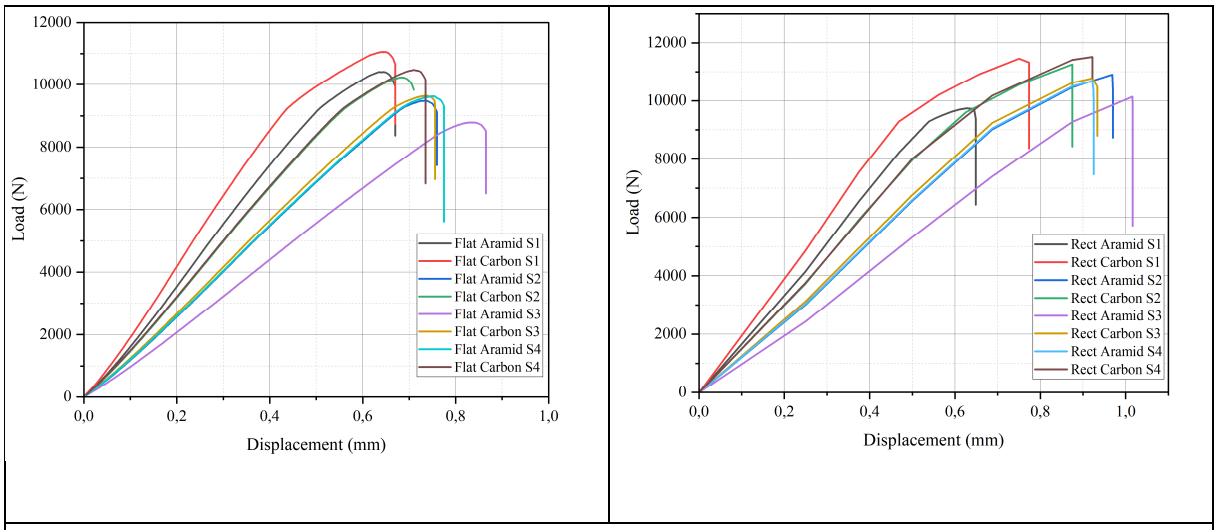

Figure 11. load-displacement curves for aluminum/composite bonded joints with flat geometry and four stacking sequences. a)Flat, b) rectangular

The results shown in Figure 12 present the combined effect of the material type and the stacking sequence on the load-bearing capacity of aluminum/composite joints, for both flat and rectangular bonding geometries. In all configurations, joints with carbon-epoxy material have a higher maximum load capacity than those with aramid/epoxy substrates, due to the greater

stiffness and strength of carbon fibers. Furthermore, the rectangular geometry noticeably improves load transfer efficiency compared to the flat configuration, particularly for carbon-epoxy, which show an increase of 4-16%, depending on the stacking sequence. This improvement is due to the greater effective bonding area and better stress redistribution in the rectangular configuration. S4 exhibits the highest load capacity among the stacking sequences for both materials and geometries, suggesting that this specific fiber orientation optimizes stress transfer at the aluminum/composite joint.

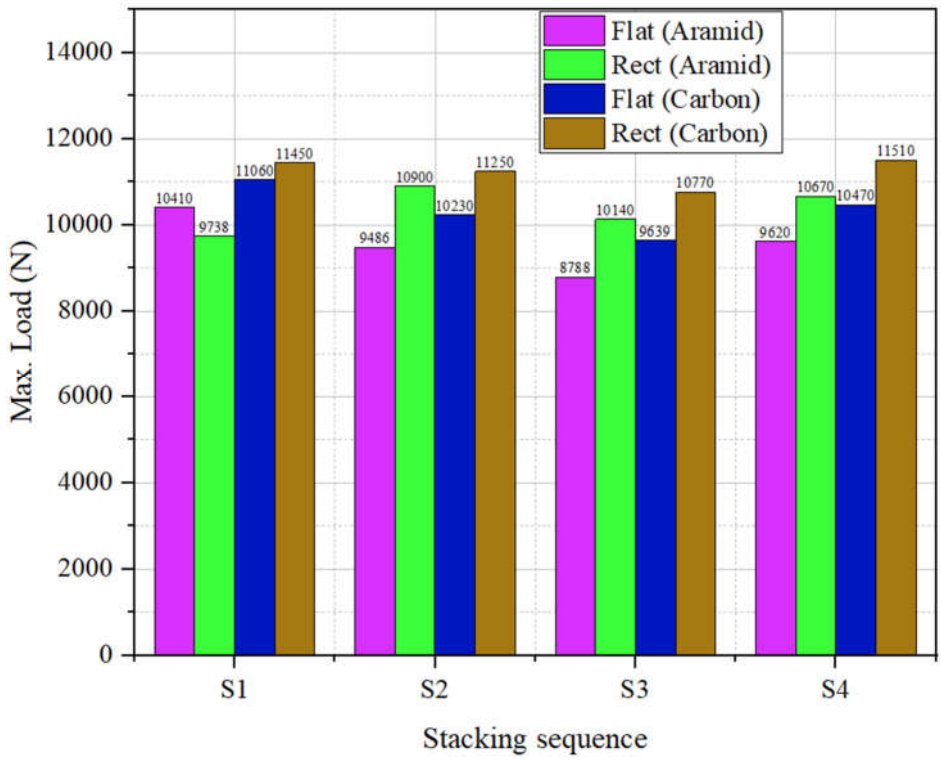

Figure 12. The maximum load comparaison for aluminum/composite joints with flat and rectangular geometries under different stacking sequences.

Effect of a semi-circular geometric modification on joint performance

In this section, a further geometric modification was added to optimize stress distribution in the adhesive layer. In this configuration, a semi-circular shape with a depth of 0.2 mm was created in the center of the external aluminum substrate surface (Figure 13). The objective is to influence the stress distribution in the bonding zone by modifying the deformation mode of the assembly. This notch improves the load transfer within the adhesive layer and delays debonding.

This can improve the overall mechanical performance and durability of the aluminum/composite assembly.

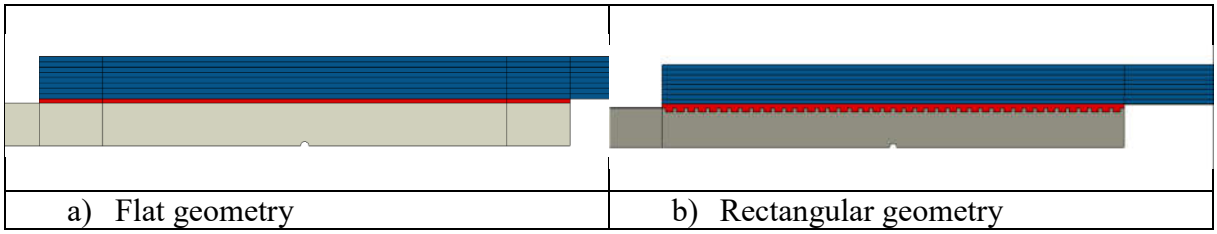

a) Flat geometry b) Rectangular geometry

Figure 13. Semi-circular notch modification added to the SLJ.

Flat geometry

Stress distribution in Aluminum/Composite bonded joint

An analysis of stress distribution in joints with modified flat bonding geometry reveals distinct behaviors between aluminum/carbon-epoxy and aluminum/aramid-epoxy assemblies. In both cases, the highest principal stresses are concentrated near the end of the overlap zone, where load transfer between the substrate of aluminum and of the composite is most critical. In the case of carbon/epoxy material, the maximum principal stress reaches approximately 637 MPa, indicating higher stiffness and load transfer. Conversely, the maximum stress of the aluminum/aramid-epoxy is lower, at approximately 563 MPa, reflecting its relatively higher energy absorption capacity (Figure 14).

The QUADSCRT damage factors provide further confirmation of this observation. In both assemblies, the regions where the criterion approaches 1 are primarily located at the end of the overlap, indicating that adhesive delamination initiates in these areas due to stress concentration. However, the extent of the critical damage zone is smaller in the aluminum/carbon-epoxy joint, indicating improved stress distribution and a delay in the initiation of deterioration compared to the aramid-epoxy configuration.

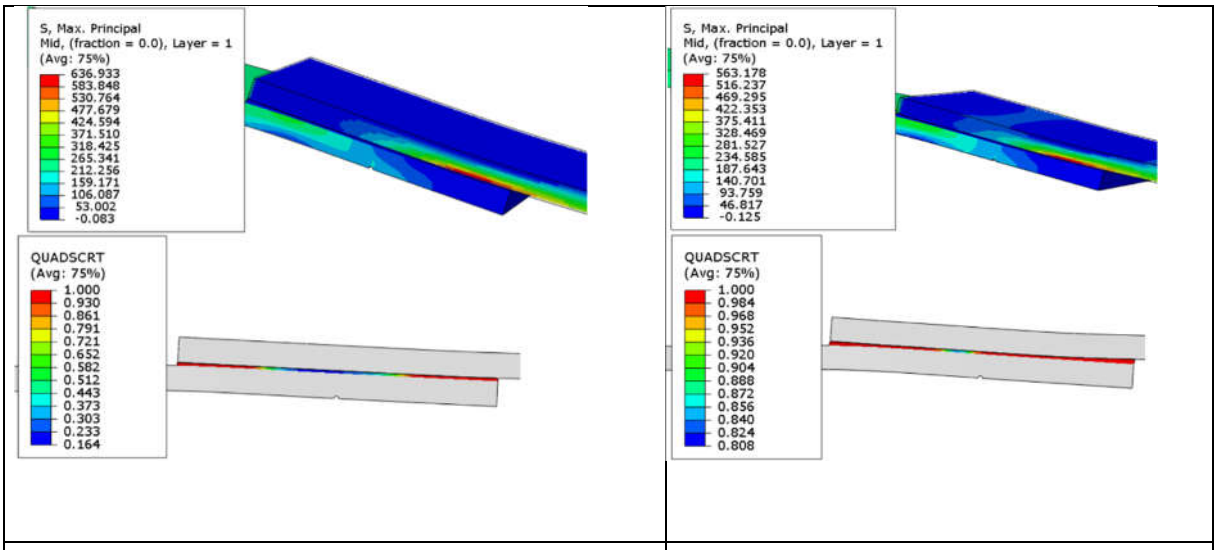

a) b)

Figure 14. Maximum principal stress and QUADSCRT damage distributions in a) aluminum/carbon-epoxy and b) aluminum/aramid-epoxy joints with modified flat geometry.

Rectangular geometry

Stress distribution in Aluminum/composite bonded joint

The figure 15 demonstrates the maximum principal stresses distribution and the damage criterion evolution (QUADSCRT) in aluminum/carbon-epoxy and aluminum/aramid-epoxy bonded joints with a rectangular overlap geometry. It is clear that the aluminum/carbon-epoxy configuration displays a more uniform stress distribution across the overlap region, with limited localized concentrations near the extremities of the joint. This enhanced distribution signifies a more efficient load transfer between the metallic substrate and the composite, consequently delaying the failure onset. Conversely, the aluminum/aramid-epoxy joint demonstrates less absorbed stress, with a more extensive damaged zone. This behavior is indicative of the reduced stiffness of the aramid-epoxy. The integration of a rectangular geometry with a carbon-epoxy substrate has been demonstrated to enhance the mechanical performance and durability of the joint.

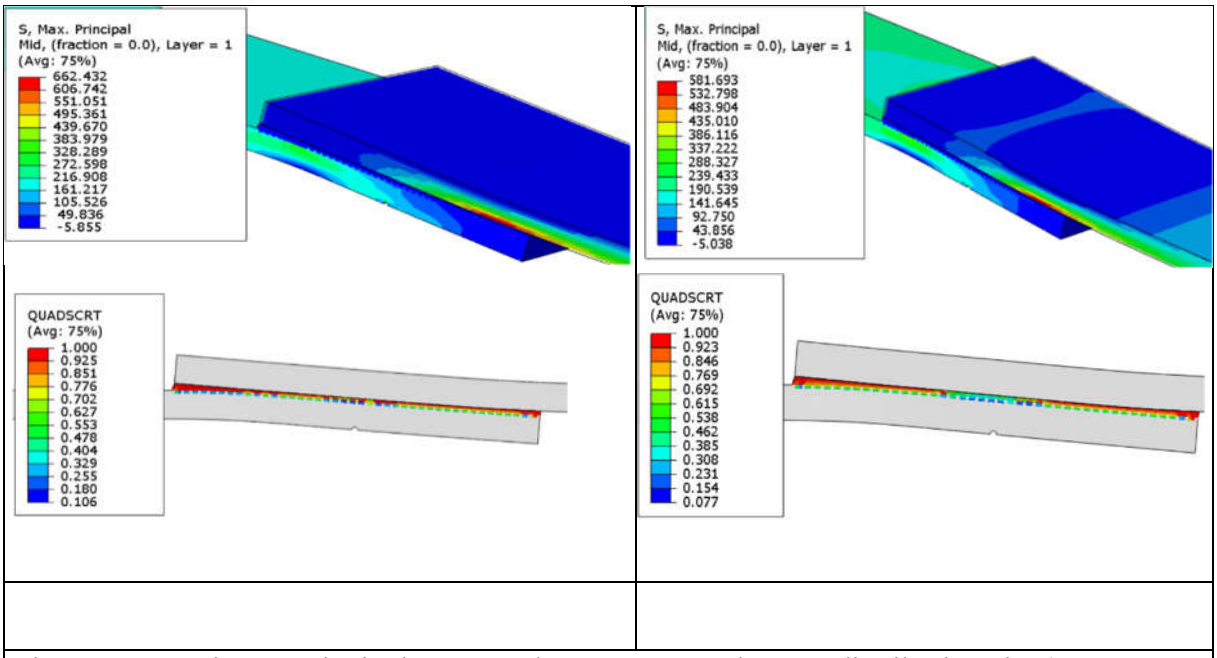

Figure 15. Maximum principal stress and QUADSCRT damage distributions in a) aluminum/carbon-epoxy and b) aluminum/aramid-epoxy joints with modified rectangular geometry.

Comparison of the results

The figure 16 illustrates the evolution of the load as a function of displacement for single-lap joints with different bonded area geometry configurations and types of reinforcement. The results demonstrate that all of the curves exhibit typical mechanical behavior, which is characterized by an initial quasi-linear phase that corresponds to the elastic response of the assembly. This is followed by a non-linear phase that reflects the progressive plasticization of the adhesive. It is evident that carbon fiber-reinforced assemblies exhibit higher load capacities in comparison to aramid-based assemblies, regardless of the geometry taken into consideration. This enhancement in performance is attributed to the higher tensile strength of carbon composites, which leads to a more uniform distribution of stresses within the overlap zone. Additionally, the bonded area geometry affects the mechanical response. Flat configurations have been shown to exhibit a marginally higher maximum load in comparison to rectangular geometries. Nevertheless, this variation remains negligible, suggesting that the geometric configuration primarily influences the local distribution of stresses rather than the overall strength of the joint.

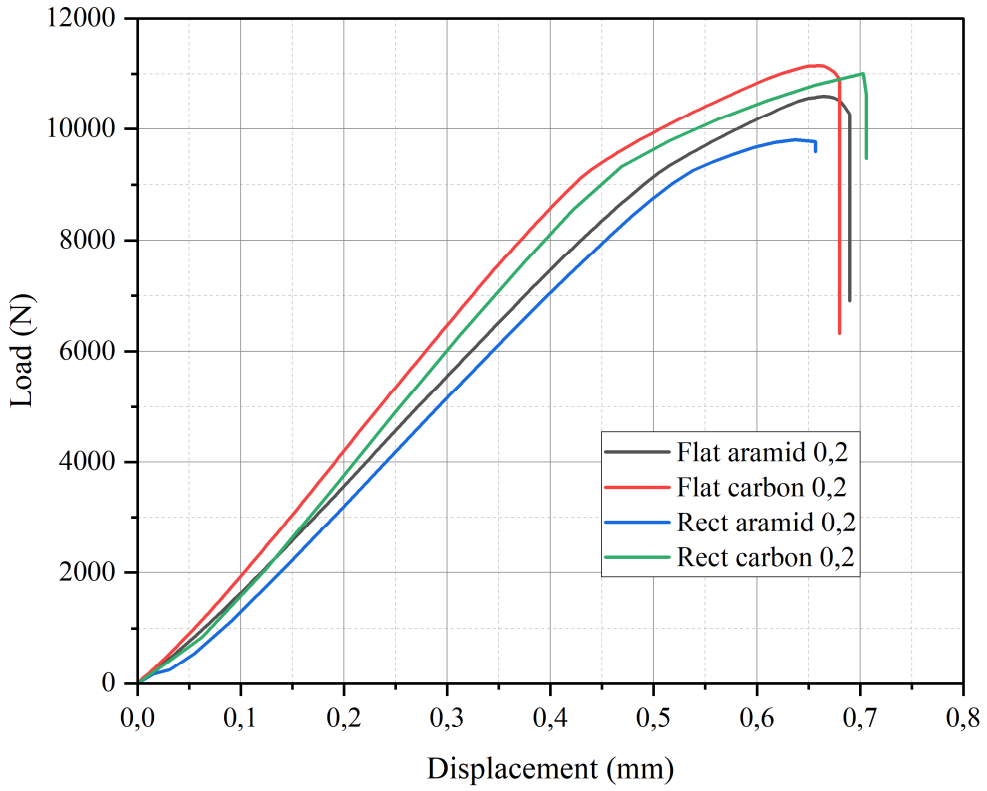

Figure 16. Load-displacement curve of single lap joints with different overlap geometries (flat and rectangular) and reinforcement types (carbon and aramid).

The figure 17 illustrates the maximum load values obtained for aluminum/composite single-lap joints, considering two overlap geometries (flat and rectangular), two reinforcement types (aramid-epoxy and carbon-epoxy), and two substrate configurations: the base model (without surface modification) and the modified model (with a semi-circular notch on the external surface of the aluminum substrate).The results reveal that Aluminum/carbon-epoxy joints achieve maximum loads that are consistently higher than Aluminum/aramid-epoxy joints, independently of geometry or configuration. The presence of a semi-circular notch has been shown to slightly improve the load-carrying capacity in the flat geometry, with an increase of +1.7% for aramid and +0.8% for carbon. This enhancement can be explained by a decrease in peel stresses at the local level and an improvement in the uniform distribution of shear stresses along the adhesive layer. Consequently, this leads to enhanced stress transfer within the overlap. Nevertheless, in the rectangular geometry, the same modification does not provide a significant advantage. Aluminum/aramid-epoxy joints demonstrated only a slight increase in strength (+0.6%), while carbon joints exhibited a marginal decrease (−3.9%).

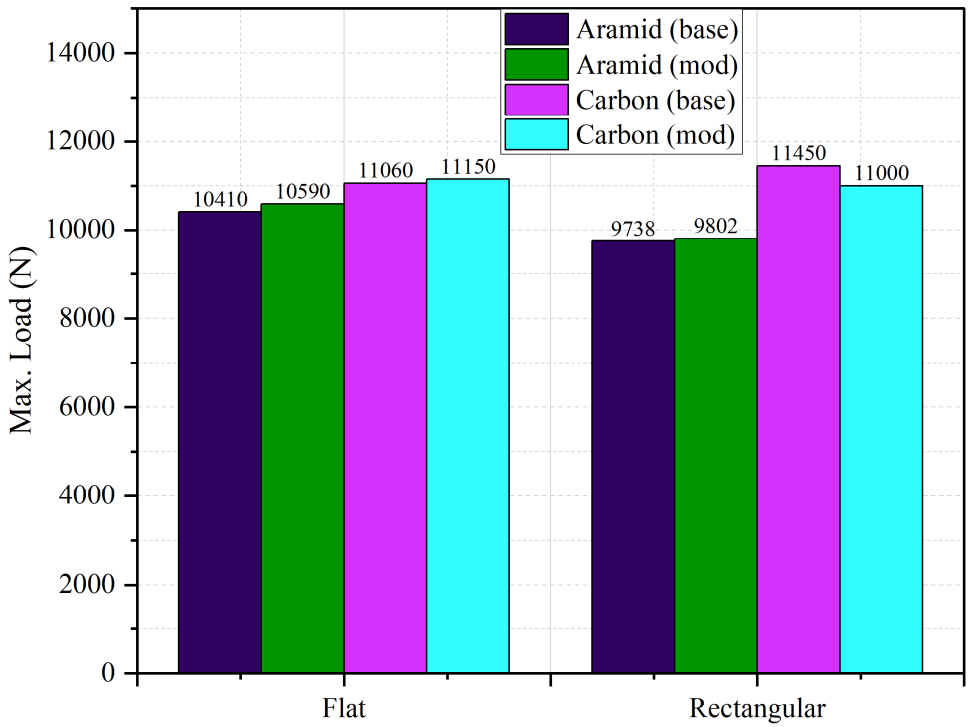

Figure 17. The effect of reinforcement type, overlap geometry and aluminum substrate modification (semi-circular notch) on the maximum load of aluminum/composite bonded joints.

Conclusion

The present study has conducted a comprehensive numerical analysis, the objective of which was to investigate the effect of bonding zone geometry, composite reinforcement type and stacking sequence on the mechanical behavior of aluminum/composite single-lap joints bonded with Adekit A140 adhesive. A 3D finite element approach implemented in Abaqus was utilized to analyze the effects of various configurations combining flat and rectangular geometries, with and without semi-circular surface modifications, on stress distribution, interfacial damage, and ultimate load capacity. The aluminum/carbon-epoxy assemblies have been shown to consistently achieve higher ultimate loads than aluminum/aramid-epoxy. This is due to the superior stiffness and load transfer efficiency of carbon fibers. However, this enhancement is associated with increased local stress concentrations in the end of the single lap joint.

The geometric configuration is also of crucial importance in the determination of joint strength and durability. The addition of a semi-circular notch in the flat geometry led to a more uniform stress distribution, resulting in slight improvements in ultimate load and delaying the onset of adhesive debonding. Conversely, the rectangular bonding geometry, despite its enhancement of load transfer and stiffness, exhibited minimal benefit from this modification. The analysis of the stacking sequence indicates that unidirectional layups $[0]_8$ exhibit the highest tensile strength by facilitating effective load transmission along the adhesive interface.

Overall, the results can be used as a basis for the design and optimization of lightweight hybrid structures in the aerospace sector. However, future work needs to include an evaluation under fatigue and environmental ageing conditions to provide a more comprehensive assessment of the durability of these optimized assemblies.

References

[1] Kim, J. S., Kim, C. G., & Hong, C. S. (2001). Practical design of tapered composite structures using the manufacturing cost concept. Composite Structures, 51(3), 285-299. https://doi.org/10.1016/S0263-8223(00)00145-8.

[2] Da Silva, L. F., & Adams, R. D. (2007). Techniques to reduce the peel stresses in adhesive joints with composites. International Journal of Adhesion and Adhesives, 27(3), 227-235. https://doi.org/10.1016/j.ijadhadh.2006.04.001.

[3] Kaye, R. H., & Heller, M. (2002). Through-thickness shape optimisation of bonded repairs and lap-joints. International journal of adhesion and adhesives, 22(1), 7-21. https://doi.org/10.1016/S0143-7496(01)00029-X.

[4] Belingardi, G., Goglio, L., & Tarditi, A. (2002). Investigating the effect of spew and chamfer size on the stresses in metal/plastics adhesive joints. International Journal of Adhesion and Adhesives, 22(4), 273-282. https://doi.org/10.1016/S0143-7496(02)00004-0.

[5] Campilho, R. D. S. G., De Moura, M. F. S. F., & Domingues, J. J. M. S. (2009). Numerical prediction on the tensile residual strength of repaired CFRP under different geometric changes. International Journal of Adhesion and Adhesives, 29(2), 195-205. https://doi.org/10.1016/j.ijadhadh.2008.03.005

[6] Simões, B. D., Nunes, P. D., Ramezani, F., Carbas, R. J., Marques, E. A., & da Silva, L. F. (2022). Experimental and numerical study of thermal residual stresses on multimaterial adherends in single-lap joints. Materials, 15(23), 8541. https://doi.org/10.3390/ma15238541

[7] Ramalho, L. D. C., Campilho, R. D. S. G., & Belinha, J. (2019). Predicting single-lap joint strength using the natural neighbour radial point interpolation method. Journal of the Brazilian Society of Mechanical Sciences and Engineering, 41(9), 362. https://doi.org/10.1007/s40430-019-1862-0

[8] BENAICHA Abdelkader, ACHACHE Habib, AMOURA Nasreddine, TOUATI BENALI Abdelaziz, & BENEFISSA Noureddine. (2026). Multi-parameter analysis of cracked aluminum pipelines repaired with composite patches. Zhuzao/Foundry, 29(5), 400–420. https://doi.org/10.29014/FJ-2026-1001-4977.89.2361

[9] Barbosa, N. G. C., Campilho, R. D. S. G., Silva, F. J. G., & Moreira, R. D. F. (2018). Comparison of different adhesively-bonded joint types for mechanical structures. Applied Adhesion Science, 6(1), 15. https://doi.org/10.1186/s40563-018-0116-1

[10] Akpinar, S., Doru, M. O., Özel, A., Aydin, M. D., & Jahanpasand, H. G. (2013). The effect of the spew fillet on an adhesively bonded single-lap joint subjected to bending moment. Composites Part B: Engineering, 55, 55-64.

https://doi.org/10.1016/j.compositesb.2013.05.056.

[11] Zielecki, W., Kubit, A., Kluz, R., & Trzepieciński, T. (2017). Investigating the influence of the chamfer and fillet on the high-cyclic fatigue strength of adhesive joints of steel parts. Journal of Adhesion Science and Technology, 31(6), 627-644. https://doi.org/10.1080/01694243.2016.1229521.

[12] Heidarpour, F., Farahani, M., & Ghabezi, P. (2018). Experimental investigation of the effects of adhesive defects on the single lap joint strength. International journal of adhesion and adhesives, 80, 128-132.https://doi.org/10.1016/j.ijadhadh.2017.08.005.

[13] Djebbar, S. C., Benyettou, M., Kouider, M., Harmel, M. W., Mohamed, B., Elajrami, M., … Campilho, R. D. S. G. (2025). Enhanced numerical modelling of damage and repair in notched 2024-T3 aluminum plates using XFEM, CZM, and VCCT. Mechanics of Advanced Materials and Structures, 1–17. https://doi.org/10.1080/15376494.2025.2476783

[14] Harmel, M. W., Kouider, M., Benyettou, M., Boussahra, M. S. N., Salma, A., Zouggar, K., & Campilho, R. D. S. G. (2025). Effect of patch geometry on the structural performance of damaged plates in bonded patch repairs techniques using a combination of XFEM and CZM techniques. *Mechanics of Advanced Materials and Structures*, 1–17. https://doi.org/10.1080/15376494.2025.2507193

[15] Harmel, M. W., Zouggar, K., Madani, K., Benyettou, M., Campilho, R. D. S. G., & Jalalvand, M. (2025). Novel concepts optimization for functionally graded adhesives used in bonded composite patch repairs techniques. *The Journal of Adhesion*, 1–30. https://doi.org/10.1080/00218464.2025.2535691

[16] Bayramoglu, S., Akpinar, S. & Çalık, A. Numerical analysis of elasto-plastic adhesively single step lap joints with cohesive zone models and its experimental verification. *J Mech Sci Technol* **35**, 641–649 (2021). https://doi.org/10.1007/s12206-021-0124-0

[17] Harmel, M. W., Zouggar, K., Benyettou, M., Madani, K., Alfano, M., & Campilho, R. D. S. G. (2026). Composite patch geometry effect on the strength of reinforced damaged plates: a numerical study. The Journal of Adhesion, 1–35. https://doi.org/10.1080/00218464.2026.2656799

[18] Silva, D. F. O., Campilho, R. D. S. G., Silva, F. J. G., & Carvalho, U. T. F. (2018). Application a direct/cohesive zone method for the evaluation of scarf adhesive joints. Applied Adhesion Science, 6(1), 13. https://doi.org/10.1186/s40563-018-0115-2.

[19] Benyettou, M., Madani, K., Djebbar, S. C., Amin, H., Belhouari, M., Elajrami, M., ... & Campilho, R. D. S. G. (2025). Analysis of load-displacement curves of an adhesive-reinforced composite patch repaired plate using the combination of XFEM and CZM techniques. *International Journal of Adhesion and Adhesives*, *136*, 103885.

[20] Araújo, I. R. S., Pinheiro, G. J. C., Rocha, R. J. B., Campilho, R. D. S. G., & Ramalho, L. D. C. (2024). eXtended Finite Element Method applied to the tensile strength evaluation of scarf adhesive joints. Procedia Structural Integrity, 54, 406-413.

https://doi.org/10.1016/j.prostr.2024.01.100.

[21] Suwanpakpraek, K., Patamaprohm, B., & Chaikittiratana, A. (2019, March). Study of adhesive bonded joint failure in composite-metal joining. In IOP Conference Series: Materials Science and Engineering (Vol. 501, No. 1, p. 012023). IOP Publishing. https://doi.org/10.1088/1757-899X/501/1/012023.

[22] Solmaz, M. Y., & Turgut, A. (2011). An experimental and numerical study on the effects of taper angles and overlap length on the failure and stress distribution of adhesively-bonded single-lap joints. Mathematical and computational applications, 16(1), 159-170.

[23] Madani, K., Touzain, S., Feaugas, X., Cohendouz, S., & Ratwani, M. (2010). Experimental and numerical study of repair techniques for panels with geometrical discontinuities. Computational Materials Science, 48(1), 83 93. https://doi.org/10.1016/j.commatsci.2009.12.005.

[24] Belhoucine, A., & Madani, K. (2022). Effect of the composite patch beveling on the reduction of stresses in 2024-T3 Aluminum structure damaged and repaired by composite, hybrid patch repair. *Structural Engineering and Mechanics*, *82*(1), 17-30. https://doi.org/10.12989/sem.2022.82.1.017.